

ChemComm

Accepted Manuscript



This is an *Accepted Manuscript*, which has been through the Royal Society of Chemistry peer review process and has been accepted for publication.

Accepted Manuscripts are published online shortly after acceptance, before technical editing, formatting and proof reading. Using this free service, authors can make their results available to the community, in citable form, before we publish the edited article. We will replace this *Accepted Manuscript* with the edited and formatted *Advance Article* as soon as it is available.

You can find more information about *Accepted Manuscripts* in the [Information for Authors](#).

Please note that technical editing may introduce minor changes to the text and/or graphics, which may alter content. The journal's standard [Terms & Conditions](#) and the [Ethical guidelines](#) still apply. In no event shall the Royal Society of Chemistry be held responsible for any errors or omissions in this *Accepted Manuscript* or any consequences arising from the use of any information it contains.

Electronic vs Structural Ordering in a Manganese(III) Spin Crossover Complex

Received 00th January 20xx,
Accepted 00th January 20xx

A. J. Fitzpatrick,^a E. Trzop,^b H. Müller-Bunz,^a M. M. Dîrtu,^c Y. Garcia,^c E. Collet^{b*} and G. G. Morgan^{a*}

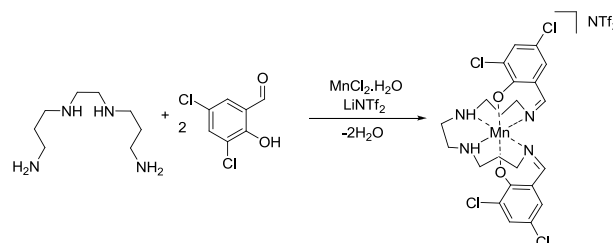
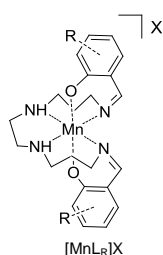
DOI: 10.1039/x0xx00000x

www.rsc.org/

A symmetry breaking spin transition in a Mn(III) complex is reported with three structural phases, a high symmetry high temperature S=2 phase, an intermediate S=1/S=2 ordered phase and an aperiodic low temperature phase with S=1 cations. The aperiodicity is interpreted as resulting from long-range ordering of the NTf₂⁻ anions.

Spontaneous symmetry breaking¹ governs many transitions in nature,² in condensed matter³ and in particle physics.⁴ Although it had been considered to explain stepped spin crossover (SCO) since the first two step transition was detected more than thirty years ago⁵ it is only in the last decade that structural symmetry breaking has emerged as a phenomenon which regularly accompanies two-step SCO in Fe(II),⁶ Fe(III)⁷ and Co(II)⁸ complexes where it is associated with long-range ordering of molecules in different spin states. In correlated systems the underlying driving force for such structural phase transitions is often magnetic frustration⁹ but despite the increasing number of symmetry breaking events in SCO complexes the origin of the phenomenon is not well understood and very likely involves competition between short-range and long-range interactions. SCO in iron and cobalt is well-known to be sensitive to lattice contents and minor changes in disorder of the ligand, anion or solvent, are sufficient to affect the thermal evolution of the moment. Although spin switching in d⁴ ions is generally more difficult to achieve¹⁰ the serendipitous discovery that complex salts of the [MnLR]⁺ series promote the effect has opened the door to systematic study of the SCO effect in manganese(III).¹¹ The geometric changes that accompany SCO in Mn(III) differ from those observed in iron both in magnitude and

direction, as the HS state in d⁴ is Jahn–Teller distorted. In addition the overall change in bond lengths is less in d⁴ than in d⁵–d⁷ ions where two electrons are promoted to the antibonding orbital set. The smaller changes which accompany the LS–HS transition should confer enhanced sensitivity of d⁴ complexes towards lattice contents, which can easily be modulated in [MnLR]⁺ by changing ligand substitution, charge balancing counterion and solvation. Such studies have thus far produced examples of HS,¹² LS^{12,13} and gradual SCO^{11–13} with one example of an abrupt and hysteretic transition which was coupled to an order–disorder transition in the PF₆⁻ counterion.¹⁴ We now report the first example of a two-step SCO in the new complex [Mn(3,5-Sal₂(323))]NTf₂, Scheme 1, which is accompanied by two structural phase transitions with an incommensurate low temperature structure.



Scheme 1: Synthesis of [MnL]NTf₂, 1.

Variable temperature magnetic susceptibility data for a polycrystalline sample of **1** was recorded between 300 – 10 K in heating and cooling modes in an applied field of 0.5 T, with an initial scan rate of 5 K/min.

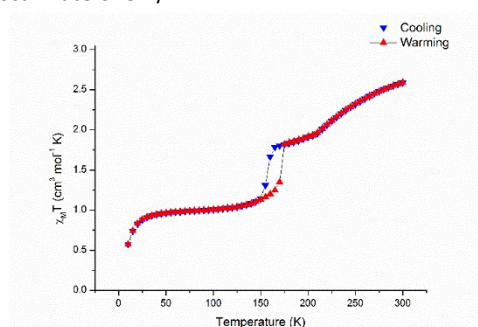


Fig. 1: $\chi_M T$ v T plot for complex **1**, showing thermal hysteresis at 5 K/min.

^aSchool of Chemistry, University College Dublin, Belfield, Dublin 4, Ireland.

^bInstitut de Physique de Rennes, Université de Rennes 1 UMR UR1-CNRS 6251, 35000 Rennes, France.

^cInstitute of Condensed Matter and Nanosciences, Molecules, Solids and Reactivity (IMCN/MOST) Université Catholique de Louvain, Place L. Pasteur 1 1348 Louvain-la-neuve, Belgium.

Email: grace.morgan@ucd.ie eric.collet@univ-rennes1.fr

Electronic Supplementary Information (ESI) available: [details of any supplementary information available should be included here]. See DOI: 10.1039/x0xx00000x

At room temperature around 75% of the sample is HS ($\chi_{\text{M}}T = 2.5 \text{ cm}^3 \text{ mol}^{-1} \text{ K}$) and the moment falls gradually on cooling, Figure 1. At 210 K the gradual decrease is arrested and the moment stabilises at around $1.6 - 1.8 \text{ cm}^3 \text{ mol}^{-1} \text{ K}$ over the temperature range 160 – 210 K suggesting a HS:LS ratio close to 1:1 in this intermediate phase (INT). Cooling below 160 K causes an abrupt collapse in the moment over a 7 K range to a $\chi_{\text{M}}T$ value of $1.0 \text{ cm}^3 \text{ mol}^{-1} \text{ K}$ which persists to 10 K (LT phase) when a further decrease due to zero field splitting is observed. On warming at 5 K/min the abrupt transition between the LT and INT phases is accompanied by opening of a 14 K hysteresis window, Figure 1.

Several reports have highlighted the importance of temperature scan rate on hysteresis width¹⁵ and in the case of **1** this was probed by a series of experiments with heating/cooling rates of 0.1, 0.5, 1.0, 2.0, 5.0 and 10 K/min. These revealed an unusual scan rate dependence in one direction only: the profile in warming mode is unaffected, but spin equilibration in cooling mode changes with scan rate, Figure 2.

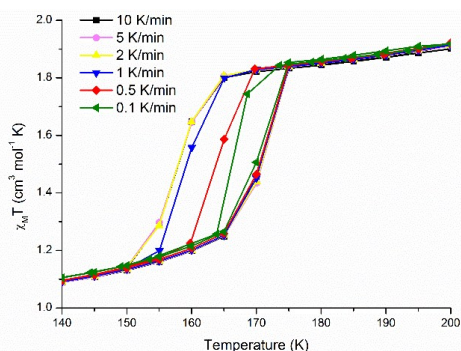


Fig. 2: Asymmetric scan rate dependence of the hysteretic window in complex **1** between 150-175 K.

In both heating and cooling modes there is no observable difference in the magnetic response when a fast scan rate is used *i.e.* the 10, 5 and 2 K/min cycles, Figure 2. At all three rates, the transition from INT to LT occurs at 157 K, Figure 2 and the switch back from the LT to the INT phase at 171 K. Slowing the scan rate to 1 K/min in cooling mode results in the transition to the LT phase occurring at slightly higher temperature, 158 K, and this pattern persists on slowing further to scan rates of 0.5 and 0.1 K/min when it increases to 164 and 167 K respectively. However in warming mode the switch from the LT to the INT phase consistently occurs at 171 K for all scan rates. This asymmetric dependence on scan rate is clearly observable in plots of $d(\chi_{\text{M}}T)/T$ versus T , Figure S.1.

Differential scanning calorimetry (DSC) data were recorded for **1** over the temperature range 105-300 K in both cooling and heating modes, at several heating/cooling rates from 1K/min to 10 K/min. Heating and cooling heat capacity profiles at selected scan rates are depicted in Figure 3. The high temperature step, which corresponds to the transition from the INT to HT phases, is always detected at 208(2) K whatever the scan rate, in agreement with SQUID and X-ray diffraction data (*vide infra*). Similarly, a temperature shift, from 157 K to 166 K, was observed for the lower branch of the hysteresis loop on reducing the scan rate from 2K/min to 1K/min, as noticed in Figure 2. A third thermal anomaly was noticed at 225 K (at 2

K/min) which is likely related to the order-disorder transition of the NTF₂⁻ anion (*vide infra*).

The total entropy obtained from the DSC study is $\Delta H_{\text{tot}} = 6.9 \text{ J mol}^{-1}$ and $\Delta S_{\text{tot}} = 37.6 \text{ J mol}^{-1} \text{ K}^{-1}$ after considering the switch in spins (75% deduced from SQUID measurements). The entropy associated with the high temperature step is $\Delta S_{\text{HT}} = 15 \text{ J mol}^{-1} \text{ K}^{-1}$ and the entropy associated to the hysteretic step is $22.6 \text{ J mol}^{-1} \text{ K}^{-1}$. Such thermal anomalies are characteristics of first order phase transitions.

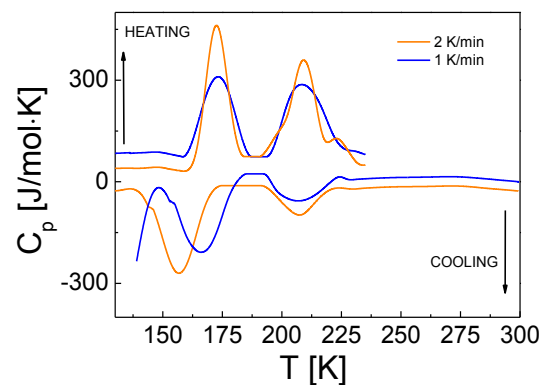


Fig. 3: DSC profiles for **1** in cooling and heating modes at selected scan rates.

Temperature dependent X-ray diffraction data also indicate a two-step conversion through the thermal evolution of the lattice parameters and intensity of the Bragg peaks, Fig. 4 and Fig. S2. A weak discontinuous change is observed around 210 K on both the cooling and warming modes. A larger discontinuous change occurs from the INT to the LT phases at 168 K on cooling and 178 K on warming. In addition, a symmetry breaking occurs in this INT phase due to a change in translation symmetry. With respect to the HT (a , b , c) cell, new Bragg peaks appear characterised by scattering vector $\mathbf{Q} = h\mathbf{a}^* + k\mathbf{b}^* + l\mathbf{c}^*$ with $k=0.5$ and $l=0.5$ (Fig. S3). The temperature dependence of these superstructure peaks indicates, in agreement with the DSC data, a weak first-order phase transition around 210 K and a stronger first-order phase transition from INT to LT phases with a thermal hysteresis (Fig. 4). The cooling branch at 168 K observed by X-ray diffraction is in agreement with magnetic measurements performed with a similar cooling rate (0.2 K/min). Crystallographic data for **1** was collected in the HT phase (210 K and 260 K), in the INT phase (185 K) and in the LT phase (120 K). A major structural rearrangement between the HT and the INT phases revealed valuable information on the relationship between the structural changes in the cell and the nature of the stepped transition in the $\chi_{\text{M}}T$ data. In the HT phase ($a=9.9941(4) \text{ \AA}$, $b=11.2766(4) \text{ \AA}$, $c=15.4647(5) \text{ \AA}$, $V=1629.38(11) \text{ \AA}^3$ at 260 K) the asymmetric unit comprises one cation and one NTF₂⁻ anion, Fig. 5. The anion is disordered around two positions in the cell. At 260 K the structure of the cation is close to the one of the HS state as characterized by the bond lengths between the Mn and the atoms bonding it to the ligand (O and N, see Table 1) with $\langle \text{Mn-L} \rangle \approx 2.038 \text{ \AA}$. The bonds most sensitive to the spin state change are the Mn-N. At 210 K the average structure of the cation shrinks and $\langle \text{Mn-L} \rangle \approx 2.013 \text{ \AA}$, Table 1.

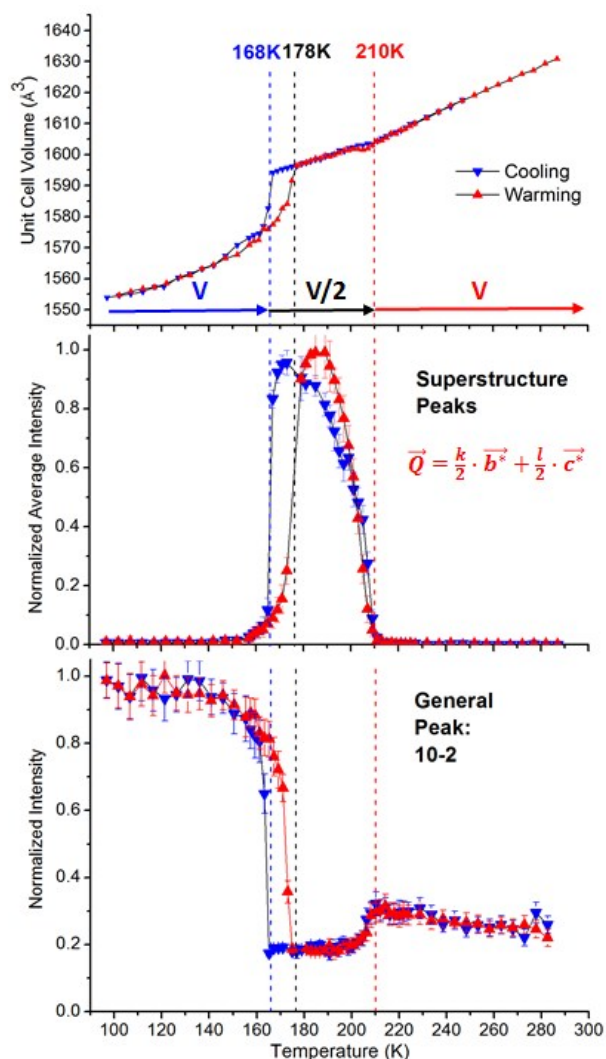


Fig. 4: Temperature dependence of the unit cell volume given in the INT cell (top), average intensity of the superstructure Bragg peaks (middle) and of the general Bragg peaks (bottom) indicating a weak first-order phase transition around 210 K and a strongly first-order phase transition around 173 K with a 10 K hysteresis width

This is due to the fact that $\approx 50\%$ of the cations are in the LS or HS states as indicated by magnetic data. The structural data indicates a doubled cell ($a=9.9196(3)$ Å, $b=20.8595(6)$ Å, $c=16.9831(4)$ Å, $V=3211.27(16)$ Å³) on the plateau, with a maximum order at 185 K, as indicated by the temperature dependence of the superstructure peaks (Fig. 4). In this doubled cell, two crystallographically independent molecular sites are observed for the cations. At 185 K cation site 1 is mainly LS, as characterized by $\langle \text{Mn}_1\text{-L} \rangle \approx 1.98$ Å and site 2 is mainly HS with $\langle \text{Mn}_2\text{-N} \rangle \approx 2.05$ Å, Table 1. The structure on the plateau is therefore made of stripes of HS and LS layers alternating in a HS-LS-HS-LS sequence along the b axis, Fig. 5, forming a spin-state concentration wave.¹⁶ The main feature of the intermediate phase is therefore the long-range ordered of cations in different electronic states. The structural analysis at 120 K revealed a more complex structure. In addition to the Bragg peaks corresponding to a unit cell similar to the HT one ($a=9.7733(3)$ Å, $b=11.0266(4)$ Å, $c=15.5654(3)$ Å, $V=1567.37(8)$ Å³) we observe satellites peaks, indexed on a 4 vector basis by: $Q=ha^* + kb^* + lc^* + mq$, h, k, l & m being integer (Fig. S3).

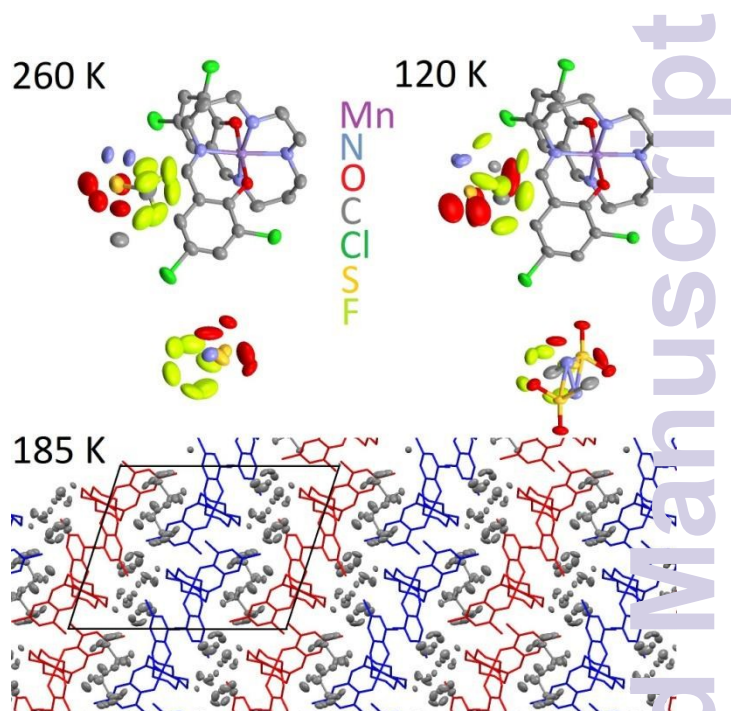


Fig. 5: View of asymmetric unit of complex 1 in the HT phase at 260 K and in the LT phase at 120 K showing the unique $[\text{Mn}(3,5\text{-ClSal}_2(323))]^+$ cation and the disordered NTf_2^- anions. In the INT at 185 K long-range order of HS (red) and LS (blue) cation layers is observed.

The modulation vector corresponds to $q = \alpha a^* + \beta b^* + \gamma c^*$ with $\alpha \approx 0.29$, $\beta \approx 0.15$ and $\gamma \approx 0.44$. As the system is triclinic there is no restriction on the orientation of the modulation vector and the 4D superspace group symmetry is $P_{-1}(\alpha\beta\gamma)$. Refining the structure in the 4D superspacegroup is beyond the scope of the present paper and the weak satellite peaks make refinement difficult. However, we can mention that in the average 3D structure we observe a significant disorder on the anions and not on the cations. This indicates that the satellites peaks are very likely due to an ordering of the anion with a modulation vector aperiodic with the average unit cell. In addition, since the LT phase is completely LS, this aperiodic order is simply of structural nature and not related to aperiodic ordering of LS and HS molecules, as recently reported in an Fe(II) SCO complex.¹⁶ At 120 K the average 3D structure of the cation is the one of the LS state as characterized by $\langle \text{Mn-L} \rangle \approx 1.98$ Å. In addition, since there is no group/subgroup relationship between the INT and the LT phase, this phase transition is reconstructive and should be first-order as experimentally observed here.

The NTf_2^- anion is well known to lower the melting point in solids due to the high degree of rotational disorder, making it a popular choice when designing ionic liquids.¹⁷ Here use of an anion with rotational freedom has assisted onset of a two-step magnetic transition with three structural phases: a HT phase with a single cation site and two positions for the disordered NTf_2^- anion; an INT phase with well-ordered crystallographically distinct cations in different electronic HS and LS states, each charge balanced by a now well-ordered NTf_2^- anion; and an incommensurate LT phase where all cations are LS and well-ordered, but where the NTf_2^- anions order with a modulation vector aperiodic with the average (a,b,c) lattice.

Table 1: Mn-Donor bond lengths for complex 1 at 120, 185, 210 and 260 K.

Temp. (K)	Bond Length (Å)			
	120	185	210	260
Z'	1	2	1	1
Mn(1)-O(1) _{phen}	1.888(3)	1.8833(17)	1.885(2)	1.884(3)
Mn(1)-O(2) _{phen}	1.888(3)	1.8906(17)	1.887(2)	1.881(3)
Mn(1)-N(1) _{im}	1.993(3)	2.001(2)	2.037(3)	2.065(4)
Mn(1)-N(4) _{im}	1.996(4)	2.001(2)	2.045(3)	2.069(3)
Mn(1)-N(2) _{am}	2.065(4)	2.0738(19)	2.132(3)	2.168(4)
Mn(1)-N(3) _{am}	2.056(3)	2.067(2)	2.123(3)	2.158(4)
Mn(2)-O(3) _{phen}		1.8801(17)		
Mn(2)-O(4) _{phen}		1.8818(17)		
Mn(2)-N(5) _{im}		2.081(2)		
Mn(2)-N(8) _{im}		2.081(2)		
Mn(2)-N(6) _{am}		2.189(2)		
Mn(2)-N(7) _{am}		2.177(2)		

Z' number of independent sites in the asymmetric unit

This work underscores the influence of structural order-disorder transitions on counterion or ligand on the switching rates in spin labile complex cations. The coupling between electronic and structural states (mainly through molecular size dependence) is at the heart of the electronic ordering in the INT phase and the anion layer (Fig. 5) plays a role. Within a cation layer, the inter-cation coupling favours a single spin state (HS or LS). However, the coupling between cations of different layers is screened by the anions (Fig. 5). Such anisotropic coupling favours layered structures and underlines the role of the anion in the formation of the striped HS-LS structure.

Notes and references

We thank the following for their generous support: Science Foundation Ireland for Investigator Project Award 12/IP/1703 (to G. M.), the National University of Ireland and the Cultural Service of the French Embassy in Ireland for scholarships (to A.J.F) and the Irish Higher Education Authority for funding a SQUID magnetometer. We also acknowledge the COST actions MP1202 and CM1305, and the Fonds National de la Recherche Scientifique for a Chargé de recherches position (to M. M. D) and FNRS for PDR T.0102.15. All authors acknowledge the generous support of University College Dublin. Structures of **1** at 120 K (CCDC no. 1404709), 185 K (CCDC no. 1404711), 210 K (CCDC no. 1404710) and 260 K (CCDC no. 1428981) deposited at the Cambridge Crystallographic Data Centre.

References

1. P. W. Anderson, *Science* **1972**, *177*, 393-396; b) S. Blundell, *Magnetism in Condensed Matter*, OUP, OXFORD, 2001, pp. 111-114; c) L. D. Landau, E. M. Lifshitz **1980**. *Statistical Physics, Part 1*. Vol. 5 (3rd ed.) Butterworth-Heinemann.
2. a) H. Hamada, C. Meno, D. Watanabe, Y. Saijoh, *Nat. Rev. Genet.*, **2002**, *3*, 103-113; b) S. F. Mason, *Nature* **1984**, *311*, 19-23.
3. a) L. E. Sadler, J. M. Higbie, S. R. Leslie, M. Vengalattore, D. M. Stamper-Kurn, *Nature* **2006**, *443*, 312-315.
4. L. Álvarez-Gaumé, J. Ellis, *Nat. Phys.* **2011**, *7*, 2-3 and references therein.
5. a) H. Köppen, E. W. Müller, C. P. Köhler, H. Spiering, E. Meissner, P. Gütllich, *Chem. Phys. Lett.* **1982**, *91*, 348-352; b) P. Gütllich, A. Hauser, H. Spiering, *Angew. Chem., Int. Ed.*, **1994**, *33*, 2024-2154;
6. a) D. Chernyshov, M. Hostettler, K. W. Törnroos, H. –B. Bürgi, *Angew. Chem., Int. Ed.* **2003**, *42*, 3825-3830; b) N. Bréfuel, H. Watanabe, L. Toupet, J. Come, N. Matsumoto, E. Collet, K. Tanaka, J. –P. Tuchagues, *Angew. Chem., Int. Ed.* **2009**, *48*, 9304-9307 c) S. Bonnet, G. Molnár, C. J. Sánchez, M. A. Siegler, A. L. Spek, A. Bousseksou, W. –T. Fu, P. Gamez, J. Reedijk, *Chem. Mater.* **2009**, *21*, 1123-1136; d) S. Bonnet, M. A. Siegler, J. S. Costa, G. Molnár, A. Bousseksou, A. L. Spek, P. Gamez, J.

- Reedijk, *Chem. Commun.* **2008**, 5619-5621; e) N. Bréfuel, E. Collet, Watanabe, M. Kojima, N. Matsumoto, L. Toupet, K. Tanaka, J. –P. Tuchagues, *Chem. Eur. J.* **2010**, *16*, 14060-14068; f) C. M. Buron-Le Cointe, N. Ould Moussa, E. Trzop, A. Moréac, G. Molnár, L. Toupet, A. Bousseksou, J. –F. Létard, G. S. Matouzenko, *Phys. Rev. B* **2010**, *81*, 214106; g) K. Nakano, S. Kawata, K. Yoneda, A. Fuyuhiko, T. Yagi, T. Nasu, S. Morimoto, S. Kaizaki, *Chem. Commun.* **2004**, 2892-2893; h) I. Nihei, H. Tahira, N. Takahashi, Y. Otake, Y. Yamamura, K. Saito, T. Oshio, *Am. Chem. Soc.* **2010**, *132*, 3553-3560; i) T. Sato, K. Nishi, S. Iijima, M. Kojima, N. Matsumoto, *Inorg. Chem.* **2009**, *48*, 7211-7229; j) K. W. Törnroos, M. Hostettler, D. Chernyshov, B. Vangdal, H. –B. Bürgi, *Chem. Eur. J.* **2006**, *12*, 6207-6215; k) M. Yamada, H. Hagiwara, H. Torigoe, N. Matsumoto, M. Kojima, F. Dahan, J. –P. Tuchagues, N. Reedijk, S. Iijima, *Chem. Eur. J.* **2006**, *12*, 4536-4549; l) V. A. Money, C. Carbonera, J. Elhaiek, M. A. Halcrow, J. A. K. Howard, J. –F. Létard, *Chem. Eur. J.* **2007**, *13*, 5503-5514; m) J. Kusz, M. Nowak, P. Gütllich, *Eur. J. Inorg. Chem.* **2013**, 832-842; n) W. Hibbs, P. J. van Koningsbruggen, A. M. Arif, W. W. Shum, J. S. Miller, *Inorg. Chem.* **2003**, *42*, 5645-5653; o) A. Lennartson, A. D. Bond, S. Piligkos, C. J. McKenzie, *Angew. Chem., Int. Ed.* **2012**, *51*, 11049-11052; p) D. L. Reger, C. A. Little, V. G. Young Jr., M. Pink, *Inorg. Chem.* **2001**, *40*, 2870-2874.
7. a) M. Griffin, S. Shakespeare, H. J. Shepherd, C. J. Harding, J. –F. Létard, C. Desplanches, A. E. Goeta, J. A. K. Howard, A. K. Powell, V. Mereacre, Y. Garcia, A. D. Naik, H. Müller-Bunz, G. G. Morgan, *Angew. Chem., Int. Ed.* **2011**, *50*, 896-900; b) B. J. C. Vieira, J. T. Coutinho, I. C. Santos, L. C. J. Pereira, J. C. Waerenborgh, V. da Gama, *Inorg. Chem.* **2013**, *52*, 3845-3850; c) Z.–Y. Li, J.–W. Dai, Y. Shiota, K. Yoshizawa, S. Kanegawa, O. Sato, *Chem. Eur. J.* **2013**, *19*, 12948-12952; d) K. D. Murnaghan, C. Carbonera, L. Toupet, M. Griffin, M. M. Dürtu, C. Desplanches, Y. Garcia, E. Collet, J. F. Létard and G. G. Morgan, *Chem. Eur. J.*, **2014**, *20*, 5613-5618.
8. a) M. G. Cowan, J. Olguín, S. Narayanaswamy, J. L. Tallon, S. Brooker, *J. Am. Chem. Soc.* **2012**, *134*, 2892-2894; b) S. Hayami, Y. Komatsu, T. Shimizu, H. Kamihata, Y. H. Lee, *Coord. Chem. Rev.* **2011**, *255*, 198-1990; c) S. Hayami, K. Murata, D. Urakami, Y. Kojima, M. Akita, K. Inoue, *Chem. Commun.* **2008**, 6510-6512; d) S. Hayami, Y. Shigeyoshi, I. Akita, K. Inoue, K. Kato, K. Osaka, M. Takata, R. Kawajiri, T. Mitani, Y. Maeda, *Angew. Chem., Int. Ed.* **2005**, *44*, 4899-4903.
9. J. P. Goff, D. A. Tennant, S. E. Nagler, *Phys. Rev. B* **1995**, *52*, 15992-16000.
10. a) P. G. Sim, E. Sinn, *J. Am. Chem. Soc.* **1981**, *103*, 241-243; b) Y. Garcia, P. Gütllich, *Top. Curr. Chem.* **2004**, *234*, 49-62.
11. G. G. Morgan, K. D. Murnaghan, H. Müller-Bunz, V. McKee, C. J. Harding, *Angew. Chem. Int. Ed.* **2006**, *45*, 7192-7195.
12. B. Gildea, L. C. Gavin, C. A. Murray, H. Müller-Bunz, C. J. Harding, G. G. Morgan, *Supramol. Chem.* **2012**, *24*, 641-653.
13. K. Pandurangan, B. Gildea, C. Murray, C. J. Harding, H. Müller-Bunz, G. G. Morgan, *Chem. Eur. J.* **2012**, *18*, 2021-2029.
14. P. N. Martinho, B. Gildea, M. M. Harris, T. Lemma, A. D. Naik, H. Müller-Bunz, T. E. Keyes, Y. Garcia and G. G. Morgan, *Angew. Chem. Int. Ed.* **2012**, *51*, 12597-12601.
15. a) F. J. Muñoz Lara, A. B. Gaspar, D. Aravena, E. Ruiz, M. C. Muñoz, N. Ohba, R. Ohtani, S. Kitagawa and J. A. Real, *Chem. Commun.*, **2012**, *4*, 4686-4688. b) M. Seredyuk, M. C. Muñoz, M. Castro, T. Romero-Morcillo, A. B. Gaspar and J. A. Real, *Chem. Eur. J.*, **2013**, *19*, 6591-6596. c) R. G. Miller, S. Narayanaswamy, J. L. Tallon and S. Brooker, *New J. Chem.*, **2014**, *38*, 1932-1941. d) R. Kulmaczewski, J. Olguín, J. A. Kitchen, H. L. C. Feltham, G. N. L. Jameson, J. L. Tallon and S. Brooker, *J. Am. Chem. Soc.*, **2014**, *136*, 878-881. e) S. Brooker, *Chem. Soc. Rev.*, **2015**, *44*, 2880-2892.
16. a) E. Collet, H. Watanabe, N. Bréfuel, L. Palatinus, L. Roudaut, L. Toupet, K. Tanaka, J. P. Tuchagues, P. Fertey, S. Ravy, B. Toudic and H. Cailleau, *Phys. Rev. Lett.*, **2012**, *109*, 257206. b) A. Marino, M. Buron-Le Cointe, M. Lorenc, L. Toupet, R. Henning, A. D. DiChiara, K. Moffat, N. Bréfuel and E. Collet, *Faraday Discuss.*, **2015**, *177*, 363-379.
17. H. Matsumoto, H. Kageyama and Y. Miyazaki, *Chem. Commun.*, **2007**, 1726-1727.-